

Ion interactions with pure and mixed water clusters

R. Maisonnay¹, M. Capron^{1,2}, S. Maclot^{1,2}, J. C. Pouilly^{1,2}, A. Domaracka¹,
A. Méry^{1,2}, L. Adoui^{1,2}, P. Rousseau^{1,2} and B.A. Huber^{1,*}

¹Centre de Recherche sur les Ions, les Matériaux et la Photonique (CIMAP) –
CEA/CNRS/ENSICAEN/UCBN, Bd Henri Becquerel, 14070 Caen, Cedex 5, France

²Université de Caen Basse-Normandie, Esplanade de la Paix, CS 14032, 14032 Caen
cedex, France

E-mail: huber@ganil.fr

Abstract. We report on collisions of highly charged Xe^{20+} ions with weakly bound clusters of water molecules and water/adenine mixtures. Singly and doubly charged water clusters are observed in the size range of $n=1$ to 65 and $n=49$ to 61, respectively. In contrast to other comparable systems, the dominant monomer fragment (H_3O^+) is formed with very low kinetic energy, hence indicating that it is formed by evaporation processes. Larger fragments are produced with larger kinetic energies due to charge-separating processes. Furthermore, water clusters are found to be protonated, only a very small amount of the non protonated dimer $(\text{H}_2\text{O})_2^+$ is observed. Excited mixed adenine/water clusters fragment by the loss of the surrounding water molecules, thus, adenine fragments are formed without water molecules attached. In addition, the adenine monomer is found to be partly protonated.

1. Introduction

Ion collisions in the gas-phase with weakly bound clusters (hydrogen- or van der Waals-bonded) may induce chemical reactions between the constituents of the cluster. This is possible due to the transfer of energy and charge during the collision which allows the system to overcome existing reaction barriers or which can create highly reactive species which interact immediately with other surrounding cluster constituents.

It has been shown experimentally, that coalescence and growth reactions occur when highly charged Xe ions collide with clusters of fullerene molecules, resulting in the formation of giant fullerenes [1]. More recently, measurements performed by the same group indicated that highly reactive C_{59}^+ fullerene ions are formed by kicking out one carbon atom from a C_{60} molecule in close He^{2+} / fullerene cluster collisions. As supported by quantum mechanical simulations the C_{59}^+ molecule reacts immediately (~ 100 fs) with one of the neighbored C_{60} molecules within the cluster forming covalently bound C_{119}^+ ions [2].

Important representatives of weakly bound clusters are water clusters which play a crucial role in different physical, chemical and biological processes on the Earth and its atmosphere. Liquid water consists of a macroscopically connected, random network of hydrogen bonds; therefore, these weakly bound aggregates of molecules have been suggested as possible transient intermediates [3]. Recently, the formation and growth of water clusters have attracted much interest [4,5] in particular as it has been shown that ion-induced nucleation plays an important role in aerosol formation and hence may influence cloud formation in the Earth's atmosphere [6-7]. Moreover, the geometrical structures of



neutral and protonated water clusters were the subject of many studies [8,9] discussing the evolution of the structure when the cluster size increases.

The fragmentation dynamics of water molecules and clusters has been studied with a large variety of electromagnetic radiations such as photons, electrons or ions [10-16] showing that high energy fragments and low energy electrons are produced. These results have direct implications on the understanding of radiation damage in living tissues. As water molecules surround all biological matter, it is important to better understand the response of water to ionizing radiation as well as to identify the influence of a water environment on the damage of the biomolecular system. By so-called indirect effects, radicals which are formed in the water environment may damage biomolecules and DNA. Ion collisions are of special importance as they are applied in cancer treatments by hadrontherapy [17].

In the present work, we report on the fragmentation of pure water clusters as well as adenine clusters embedded in a water environment, induced in gas phase collisions by multiply charged ions (Xe^{20+}).

2. Experimental approach

Ion-cluster collisions are studied in a crossed beams device, the set-up of which is shown in the figure 1. It is described in more detail in a previous communication [18]. In brief, multiply charged ions in different charge states (1-25) are produced in an electron cyclotron resonance ion source (ECRIS) of the installation ARIBE at the GANIL facility [19]. At acceleration voltages between 10 and 20 kV, the ions are mass-selected and guided to the interaction region. They cross a beam of neutral hydrogen-bonded or van der Waals bonded clusters, which have been produced within a cluster aggregation source [20]. The cluster beam is characterized by a wide mass distribution (containing up to ~65 molecules) at a cluster temperature of ~70 K. After the pulsed ion beam (typical pulse width 500 ns, frequency of the order of 2 kHz) has passed the interaction zone, cationic interaction products are extracted and mass-over-charge analyzed by means of a time-of-flight mass spectrometer, from which secondary ion mass spectra are obtained. The spectrometer acceptance allows for 100% detection of fragments with kinetic energies of up to 10 eV; higher energies will provoke forward- and backward-structures in the peak forms. Due to the strong post-acceleration (up to 25 kV) of the ions towards an electron emitting conversion plate, the detection efficiency is constant also for large fragment masses. Time-of-flights can be recorded in an event-by-event mode allowing to analyze correlations between fragments [21].

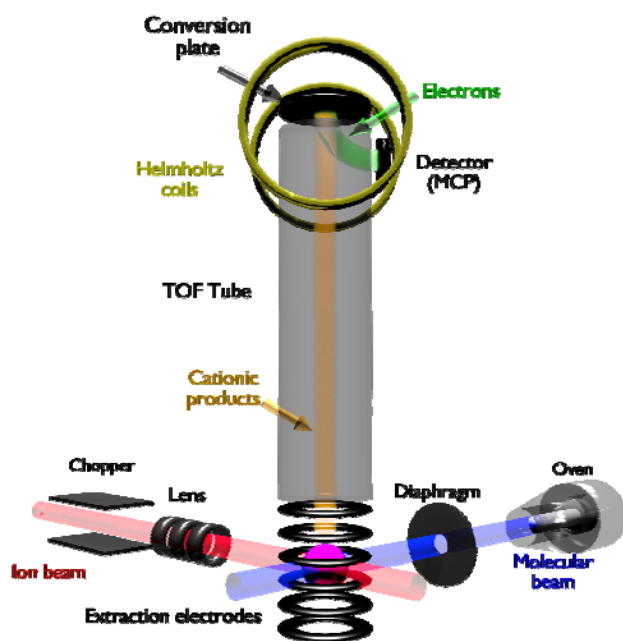


Figure 1: Experimental device with crossed ion and molecular beams and the time-of-flight mass spectrometer.

3. Ion interactions with neutral water clusters

In figure 2 we show an inclusive mass spectrum (containing all events) obtained in collisions of Xe^{20+} projectiles at 300 keV with a wide distribution of neutral water clusters $(\text{H}_2\text{O})_n$, with n between 1 and ~ 65 . The neutral molecules are ionized by electron capture processes, forming during the collision time (~ 10 fs) singly and multiply charged water clusters. The observed peak intensities of the protonated water clusters (see discussion below), measured on a time scale of several μs , decrease with increasing cluster size showing the dominance of small size clusters and fragments. The slightly increased relative intensity for $n=4$ reflects the higher stability of the ‘magic number’ cluster.

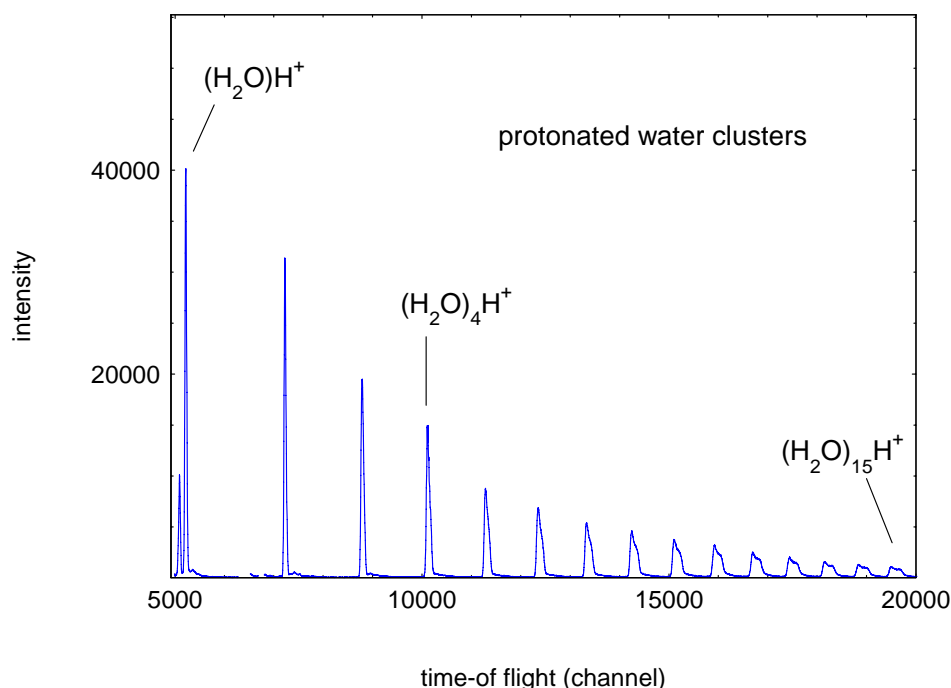
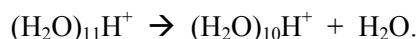


Figure 2. Mass spectrum of protonated water clusters formed in collisions of 300 keV Xe^{20+} ions with neutral water clusters (corrected for N_2 and O_2 background).

Ionized excited clusters may decay by evaporation of a neutral water molecule or via evaporation sequences or by charge-driven fission processes. In the first case, the kinetic energies of the emitted molecules and of the residual ion are rather small in the meV energy range. After evaporation of several molecules, the residual ion may accumulate larger recoil energies in the range of several hundreds of meV. Finally, in charge driven reaction, due to the Coulomb repulsion, kinetic energies in the eV range are typical values which will strongly influence the shape of the measured peaks in particular by increasing their half widths.

In figure 3 more details are given concerning the variation of the peak form with cluster size. In the left upper panel, it is shown that the peak width of small fragments (or cluster residues) increases strongly with size n also showing a tail to higher masses. As shown more clearly in the right upper panel of figure 3 for the cluster with $n=10$, the widening is due to the kinetic energy release upon fragmentation, which is in the present case of the order of 2 eV as determined by the peak width [22]. The dashed curve is the result of a SIMION trajectory calculation within the time-of-flight mass spectrometer, taking into account a 4π emission angle of the fragment, an energy distribution of 2 eV with a half width of 250 meV, as well as the special detector geometry leading to an asymmetric form. The tail towards larger drift times is due to retarded evaporation processes which occur within the extraction field, i.e. on a μs time scale:



In the intermediate cluster size range (left lower panel of figure 3) we observe the formation of doubly charged water clusters. Whereas in the literature the appearance size for doubly charged species has been reported to be > 35 [23], here we observe these systems in the size range from about $n=41$ to 61. The upper limit is close to the maximum cluster size in the primary distribution and agrees with the limit for singly charged systems in the spectrum.

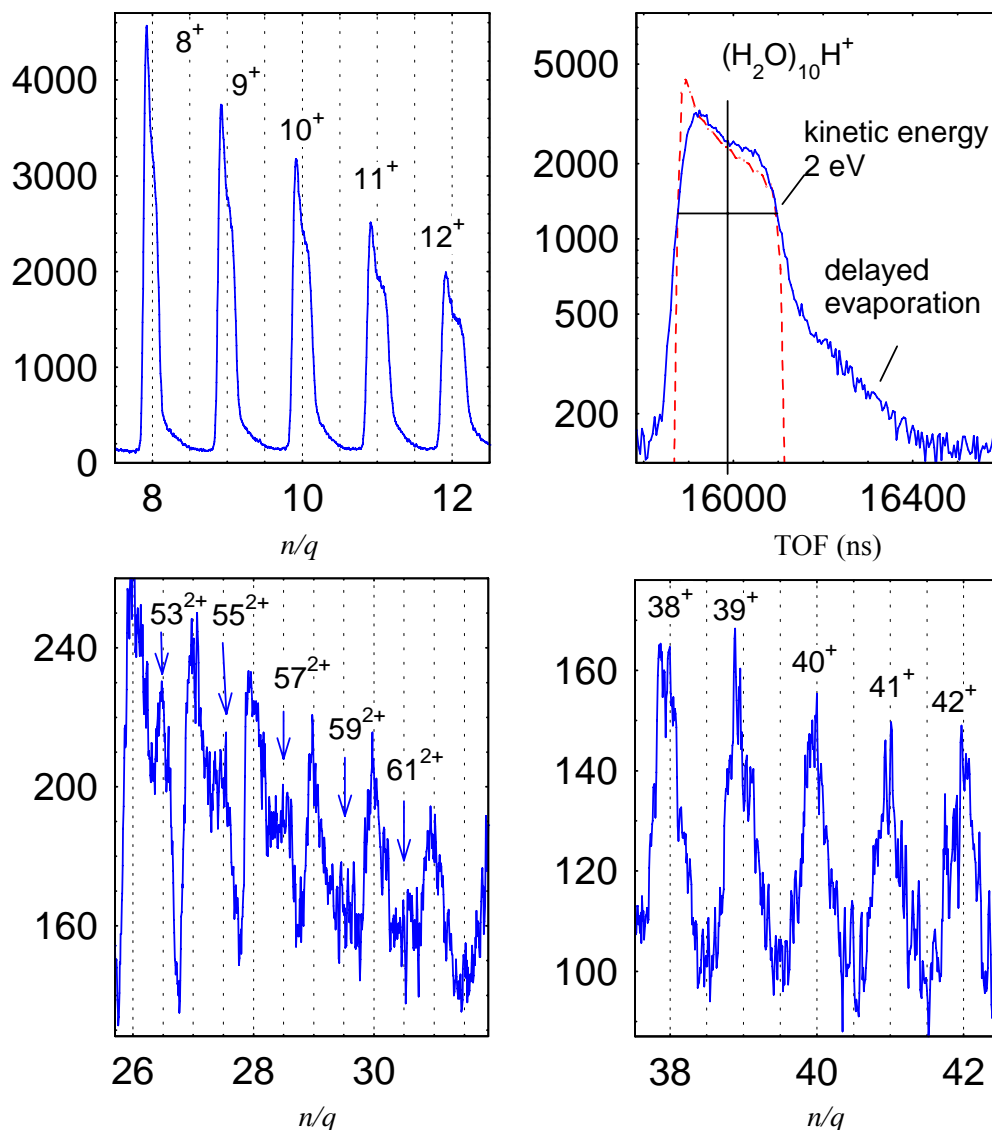


Figure 3. Details of the mass spectrum in regions of different cluster sizes. The dashed line in the upper right panel is the result of trajectory calculations of the $(\text{H}_2\text{O})_{10}\text{H}^+$ ion with a kinetic energy of 2 eV.

The lower right panel of figure 3 shows symmetric peak structures for larger clusters, corresponding to kinetic fragment energies below 1 eV. An overview of the most likely kinetic energies of the fragments is given in Table 1. The kinetic energy increases with cluster size, passes a maximum and decreases again. It is surprising that the average kinetic energy of the monomer H_3O^+ is that low. In the case of asymmetric fission processes, we would expect a much larger energy release as it is the case for other weakly bound cluster systems like clusters of fullerenes, PAHs or biomolecules,

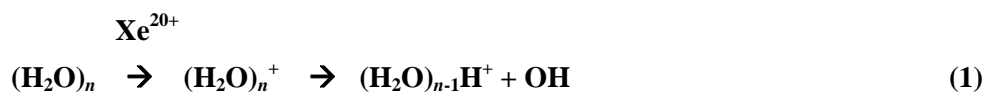
where in general a wide monomer peak is observed in the fragmentation spectrum [24-26]. Hence, it is likely that the small fragments are formed by evaporation processes. In the intermediate range ($10 < n < 20$) the kinetic energies are of the order of 2 eV indicating the importance of charge driven processes. This finding is confirmed by experiments with He^{2+} ions, which produce water clusters in lower average charge states. Here, the kinetic energy of clusters in the intermediate size range is reduced by a factor of 2. When we analyse spectra where only multiply charged water clusters are formed (so-called multistop spectra) the kinetic energy of the monomer increases to about 1 eV reflecting Coulomb repulsion. Furthermore, high energy H^+ fragments are observed (with average kinetic energies between 15 and ~ 20 eV) proving the fragmentation of individual water molecules when the system is highly charged.

Table 1. Average kinetic energies of fragments produced in collisions of Xe^{20+} ions with neutral water clusters as a function of their size.

cluster size n	kinetic energy (eV)
1	0.19
3	0.38
5	0.9
10	2.0
20	2.2
41	0.8

As mentioned above, the observed clusters are protonated. Similar results have been obtained in other experiments using 26.5 eV soft X-ray laser [4], fs photoionization [10], chemical ionization [27], electron impact ionization [28] and more recently high energy ion impact [12]. In an experimental study performed with mixed $\text{Ar}(\text{H}_2\text{O})_n$ clusters [29], ionized by photon collisions close to the ionization threshold (photon energies of 11.62 and 11.83 eV), also unprotonated radical cations have been observed for small cluster sizes ($n < 10$). The finding was explained by the emission of the Ar atom after ionization which is supposed to cool the cluster and to stabilize the radical cations.

The observed protonated species are likely to be produced by a fast proton transfer reaction and the loss of OH involving two molecules of the cluster following the ionization process, along the following equation:



This fast reaction can be followed by the evaporation of further water molecules, depending on the internal energy of the system. Recently it has been shown by TD-DFT Car Parinello calculations that this transfer proceeds on a very short timescale namely within less than 1 ps [12,30]. This is shorter than the average statistical dissociation time.

Although in ionizing collisions with highly charged ions the transferred energy can be as low as 1 eV for single ionization, our results indicate that the potential energy barrier for protonation of water clusters is lower than this value. Thus, we observe radical cations only for $n=1$ and $n=2$, whereby for $n=2$ the intensity is very low (see figure 4). It should be noted that some of the water monomer radical cations observed can come from residual gas in the spectrometer extraction region.

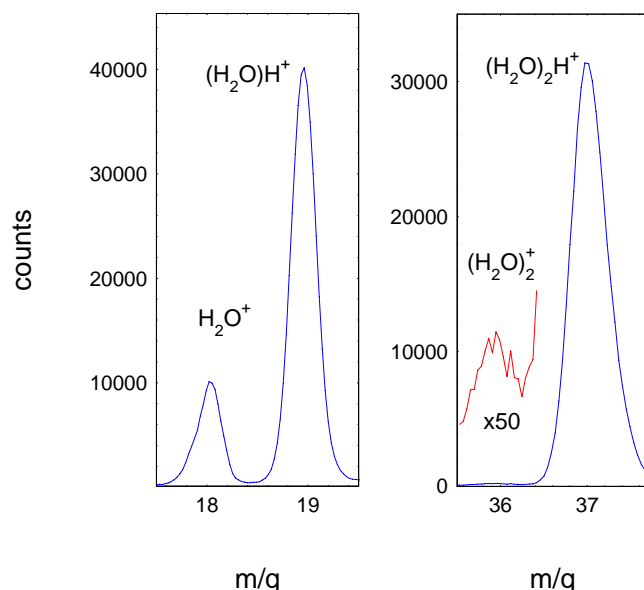


Figure 4: Protonated species and radical cations formed in collisions of Xe^{20+} with $(\text{H}_2\text{O})_n$ at a collision energy of 300 keV. Note the low intensity of $(\text{H}_2\text{O})_2^+$. For larger n values only protonated clusters are observed.

4. Mixed adenine-water clusters

In the following we will describe collision experiments performed with mixed clusters containing water molecules as well as molecules of the nucleobase adenine. These targets are prepared in the cluster aggregation source by introducing water vapor and creating an adenine vapor pressure by heating an oven device. In figure 5 we show a series of mass spectra obtained after collisions of Xe^{20+} projectiles at 300 keV with different mixed cluster distributions (temperatures of the adenine oven are given). At very low temperatures (upper left panel) we find a spectrum of pure water clusters as described in the section above (figure 2, the peak forms are different in both spectra due to a modified time-of-flight system).

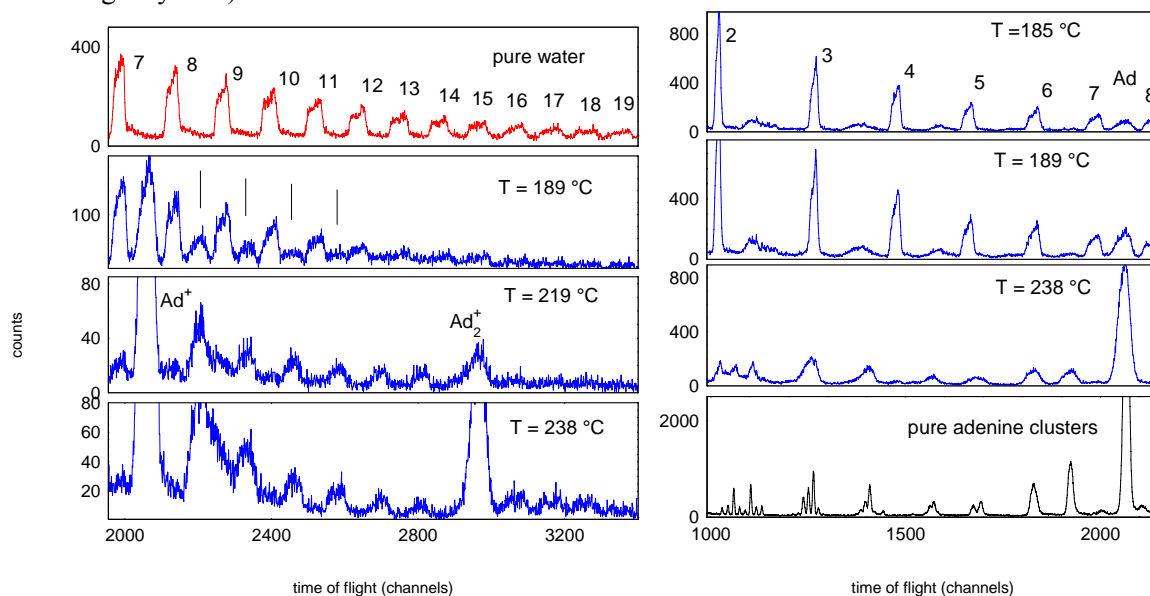


Figure 5. Inclusive mass spectra obtained in Xe^{20+} collisions with water, adenine and mixed water-adenine clusters. The given temperatures are those of the adenine oven and reflect the adenine vapor pressure in the cluster source. Left: mixed cluster distribution; right: fragmentation region of the adenine molecule.

At higher temperatures ($T=189^\circ\text{C}$) we observe in addition to water clusters the adenine monomer peak between $(\text{H}_2\text{O})_7\text{H}^+$ and $(\text{H}_2\text{O})_8\text{H}^+$ as well as a series of hydrated adenine clusters. At even higher temperatures no water clusters are observed anymore, the spectrum contains only adenine and hydrated adenine clusters ($T=238^\circ\text{C}$) with up to 8 water molecules attached. The neutral target might contain even more water molecules as evaporation processes, as discussed above, are expected to occur. The relative integrated intensities (see figure 6) decrease with the number of attached water molecules in the cluster and are more or less independent of the fact whether the adenine monomer or dimer is present.

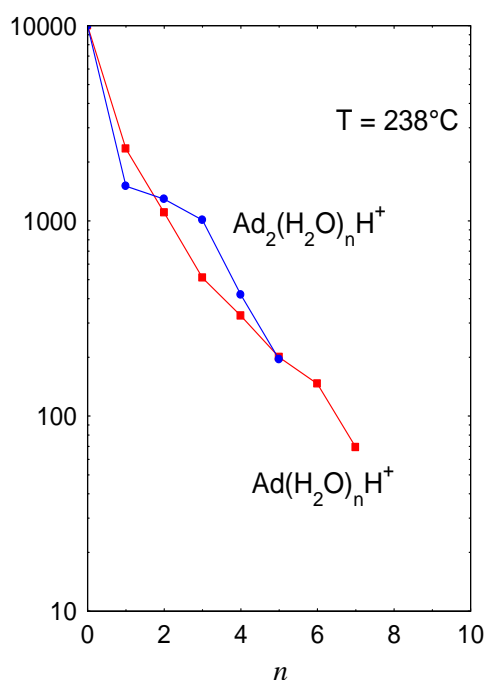


Figure 6: Relative intensities of hydrated adenine clusters.

On the right panel of figure 5, the mass range below the adenine monomer is shown. When comparing the fragmentation of adenine and hydrated adenine, the same types of fragments are observed. In particular, no fragments where water molecules are attached are produced, indicating that all water molecules are lost before the adenine molecule fragments. This is due to the fact that the fragmentation of the adenine molecule requires more energy than the evaporation of a water molecule. This is in agreement with studies of the collision induced dissociation of nanosolvated AMP⁻ anions, where the loss of water molecules turned out to be the dominant de-excitation mechanism [31].

In experiments with low charged projectiles (O^{3+} at 37.2 keV) [32], we analyzed the peak form of the adenine peak in more detail. In figure 7 we compare the peak shape of the adenine monomer for different targets: In the case of the isolated adenine molecule the peak is rather narrow showing the isotopic distribution as well as the loss of one hydrogen atom. When adenine clusters are irradiated, the peak becomes wider due to evaporation and fragmentation processes. Finally, when using hydrated adenine clusters, the peak becomes even wider and shifts slightly to larger masses. A peak deconvolution shows that the adenine fragment ion is formed partly in its protonated form, which might be explained by a proton transfer from the protonated water to the adenine.

We know, as discussed above in section 3, that when the O^{3+} ion interacts with a water molecule in the hydrated cluster of adenine, a protonated water molecule is fastly formed by the emission of a neutral OH fragment on the picosecond time scale. As the proton affinity of the adenine molecule is higher than that of water [40, 41], a proton transfer to the adenine molecule may occur. Finally, after evaporation of all surrounding water molecules the protonated adenine monomer (AdH^+) is observed.

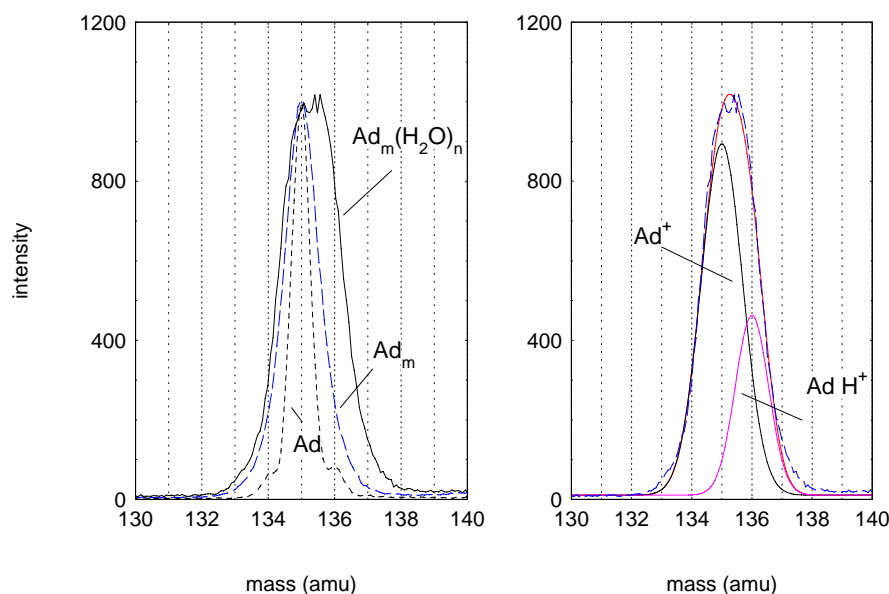


Figure 7. Left: shape of the adenine peak obtained in ion collisions with the isolated adenine molecule (short dashed line); with adenine clusters (long dashed line) and hydrated adenine clusters (full line). Right: deconvolution of the peak obtained with hydrated adenine clusters yielding pure adenine as well as protonated adenine monomers (see also ref. 32).

5. Acknowledgements

The experimental studies have been performed at the ARIBE facility, the low-energy ion facility of GANIL. Financial support received from the ANR Programme Blanc PIBALE/ANR-09-BLAN-013001 and the Conseil Régional de Basse-Normandie is gratefully acknowledged.

References

- [1] Zettergren H, Schmidt H T, Jensen J *et al.* 2010 *J. Chem. Phys.* **133**, 104301
- [2] Zettergren H, Rousseau P *et al.* 2013 *Phys. Rev. Lett.* submitted
- [3] Stillinger F H 1980 *Science* **209**, 4455
- [4] Dong F *et al.* 2006 *Chem. Phys.* **124**, 224319
- [5] Zamith S, Feiden P, Labastie P *et al.* 2010 *Phys. Rev. Lett.* **104**, 103401
- [6] Svensmark H, Bondo T and Svensmark J 2009 *Geophys. Res. Lett.* **36**, L15101
- [7] Hvelplund P *et al.* 2010 *Int. J. Mass Spectrom.* **292**, 48
- [8] Ludwig R 2004 *ChemPhysChem* **5**, 1495
- [9] Zwier T S 1999 *Science* **304**, 1119
- [10] Radi P P *et al.* 1999 *J. Chem. Phys.* **111**, 512
- [11] Sternovski Z *et al.* 2001 *Phys. Rev. A* **64**, 023203
- [12] Adoui L *et al.* 2009 *J. Phys. B: At. Mol. Opt. Phys.* **42**, 075101
- [13] Alvarado F, Hoekstra R *et al.* 2005 *J. Phys. B: At. Mol. Opt. Phys.* **38**, 4085
- [14] Legendre S *et al.* 2005 *J. Phys. B: At. Mol. Opt. Phys.* **38**, L233
- [15] Adoui L *et al.* 2001 *Phys. Scr.* **T92**, 89
- [16] Kumarrapan V *et al.* 2003 *Phys. Rev. A* **67**, 063207
- [17] Krämer M *et al.* 2000 *Phys. Med. Biol.* **45** 3299
- [18] Bergen T, Biquard X, Brenac A *et al.* 1999 *Rev. Sci. Instrum.* **70**, 3244
- [19] Bernigaud V, Kamalou O, Ławicki A, *et al.* 2008 *Publ. Astron. Obs. Belgrade* **84**, 83
- [20] Chandezon F, Huber B A and Ristori C 1994 *Rev. Sci. Instrum.* **65**, 3344
- [21] Capron M *et al.* 2012 *Chem. Eur. J.* **18**, 9321
- [22] Tomita S *et al.* 2002 *Phys. Rev. A* **65**, 053201

- [23] Shukla A K, Moore C and Stace A J 1984 *Chem. Phys. Lett.* **109**, 324
- [24] Manil B, Maunoury L, Huber B A *et al.* 2003 *Phys. Rev. Lett.* **91**, 215504
- [25] Holm A I S , Zettergren H, Johansson H A B *et al.* 2010 *Phys Rev Lett.* **105**, 213401
- [26] Maclot S *et al.* 2011 *ChemPhysChem* **12**, 930
- [27] Shi Z *et al.* 1993 *J. Chem. Phys.* **99**, 8009
- [28] Echt O *et al.* 1984 *Chem. Phys. Lett.* **108**, 401
- [29] Shinohara H and Nishi N 1986 *J. Chem. Phys.* **84**, 5561
- [30] Gaigeot M P *et al.* 2007 *J. Phys. B: At. Mol. Opt. Phys.* **40**, 1
- [31] Liu B, Nielsen S B, Hvelplund P *et al.* 2006 *Phys. Rev. Lett.* **97**, 133401
- [32] Domaracka A, Capron M, Maclot S *et al.* 2012 *J. Phys.: Conf. Series* **373**, 012005